ENDOR study of 14N hyperfine and quadrupole couplings of $N_2D_4^{\cdot+}$ formed in deuterated $Li(N_2H_5)SO_4$ single crystal

ARTICLE *in* THE JOURNAL OF PHYSICAL CHEMISTRY A · MARCH 2002

Impact Factor: 2.69 · DOI: 10.1021/jp0125303

4 AUTHORS, INCLUDING:

Audun Sanderud
Norwegian Radiation Protection Authority
29 PUBLICATIONS **169** CITATIONS
SEE PROFILE

Einar Sagstuen
University of Oslo
176 PUBLICATIONS **2,393** CITATIONS
SEE PROFILE

Anders Lund
Linköping University
287 PUBLICATIONS **3,222** CITATIONS
SEE PROFILE

ENDOR Study of ^{14}N Hyperfine and Quadrupole Couplings of $N_2D_4^{\bullet+}$ Formed in Deuterated $Li(N_2H_5)SO_4$ Single Crystal

Yoshiteru Itagaki,*,† Audun Sanderud,‡ Einar Sagstuen,‡ and Anders Lund§

Department of Materials Chemistry, Graduate School of Engineering, Hiroshima University, Higashi-Hiroshima, 739-8527 Japan, Department of Physics, University of Oslo, P.O. Box 1048 Blindern, N-0316 Oslo, Norway, and Department of Physics and Measurement Technology, Linköping University, S-581 83 Linköping, Sweden

Received: July 3, 2001; In Final Form: November 16, 2001

X-irradiated $Li(N_2D_5)SO_4$ single crystals were investigated using EPR and ENDOR spectroscopy. The ^{14}N-ENDOR spectra of the deuterated hydrazine radical cation $N_2D_4^{\bullet+}$ were clearly observed at 240 K. ^{14}N hyperfine (hfc) and nuclear quadrupole (nqc) tensors of the $N_2D_4^{\bullet+}$ cation were determined from angular variation ENDOR measurements in the three orthogonal planes of the crystal. The hfc tensor obtained for the two equivalent ^{14}N atoms is very close to that reported in a $N_2H_5HC_2O_4$ single crystal, and the present results support the previous conclusion that the cation has a planar structure at 240 K. The ^{14}N nqc tensor was estimated using semiempirical methods and also calculated from the field gradients in the LiHzS crystal as evaluated by density functional theory methods. The general agreement with experimental observations further supported the suggested geometrical structure of the $N_2H_4^{\bullet+}$ radical. The ^1H and ^{14}N-ENDOR enhancements observed may be due to weakened dipolar interactions between $^{14}N-^2D$ and $^1H-^2D$ leading to increased T_{1n} relaxations of the ^{14}N and residual ^1H nuclei of the $N_2D_4^{\bullet+}$ cation (and/or other isotopomers) in the deuterated crystals as compared to those in the $Li(N_2H_5)SO_4$ crystals.

Introduction

The $Li(N_2H_5)SO_4$ (abbreviated as LiHzS hereafter) crystal is known to be a good proton conductor, and the conductivity is highly anisotropic: along the *c* axis it is 10^3 times higher than that in the *a*−*b* plane at room temperature.[1] Since this discovery, many efforts have been made to clarify the physical properties of the crystal.[2−9]

Hilczer et al.[8] reported that γ-ray irradiation of the LiHzS crystal reduces the proton conductivity concomitantly with the partial destruction of the N−H···N conduction chain along the *c*-axis direction. Recently, we reported that this destruction of the conduction chain is caused by a formation of a $N_2H_4^{\bullet+}$ cation in the X-irradiated crystal.[9] In that study, the ENDOR (electron nuclear double resonance) method combined with EPR was successfully applied to evaluate the ^1H-hyperfine coupling (hfc) tensors of the $N_2H_4^{\bullet+}$ cation with high accuracy. Furthermore, a molecular distortion of the cation below 230 K was suggested. However, the ^{14}N-ENDOR signals from the $N_2H_4^{\bullet+}$ cation were not observable in the LiHzS crystal, probably because of rapid spin relaxation of the ^{14}N nucleus. In the previous work,[9] the powder EPR spectrum of the cation in the LiHzS was successfully simulated by using ^{14}N-hyperfine coupling reported for the identical cation produced in $N_2H_5HC_2O_4$ single crystals.[10] EPR studies of this radical species in other single-crystal systems have led to the wrong assignment[5] because of the many lines present in the spectra, a total of 20 736, when all transitions are taken into account. ENDOR is the only practical method for a correct identification under such circumstances. ^1H-ENDOR spectra in the $N_2H_5HC_2O_4$ single crystals were observed by Sagstuen et al.,[11] and the ^1H hfc tensors agree well with those determined in LiHzS. However, no ^{14}N hfc and nuclear quadrupole coupling (nqc) tensors were reported in that study. To validate the structure and the orientation of the $N_2H_4^{\bullet+}$ cation formed in the LiHzS crystal, which takes an important role for the conductivity loss, it is desirable to determine the precise ^{14}N hfc and nqc tensors as well as ^1H hfc tensor. In particular, the nqc is expected to be observed in the ^{14}N-ENDOR spectrum. This coupling may provide useful information on the local electric field gradient or charge distribution in the crystal. So far, ^7Li and ^2D, but not ^{14}N, quadrupole couplings have been measured by NMR techniques during investigations on the phase transition of the LiHzS crystal.[12] ^{14}N nqc has, however, been observed with ENDOR in a variety of irradiated single crystals.[13−16]

In the present study, clear ^{14}N-ENDOR signals were successfully obtained by replacing the hydrogens of LiHzS with deuterium (LiDzS), and the ^{14}N hfc and nqc tensors of the $N_2H_4^{\bullet+}$ cation ($N_2D_4^{\bullet+}$ in the LiDzS) were determined. In addition, the ^{14}N nqc tensor was estimated using semiempirical methods and also calculated from the field gradients in the LiHzS crystal as evaluated by the DFT (density functional theory) method to be compared with the experimental results obtained from the LiDzS single crystals.

Experiment and Calculation

Single crystals of LiDzS were prepared by crystallization from saturated LiHzS/D_2O solutions by slow evaporation at room temperature. The crystals obtained were recrystallized up to four times in 99% D_2O to obtain deuterium-enriched crystals. The LiDzS crystal is orthorhombic with space group $Pna2_1$,[3] being elongated along the *c* axis similarly with the LiHzS crystal.

* To whom correspondence should be addressed. E-mail: yoita@hiroshima-u.ac.jp. Phone: +81-824-24-7737. Fax: +81-824-22-7191.
† Hiroshima University.
‡ University of Oslo.
§ Linköping University.

10.1021/jp0125303 CCC: $22.00
Published on Web 02/26/2002

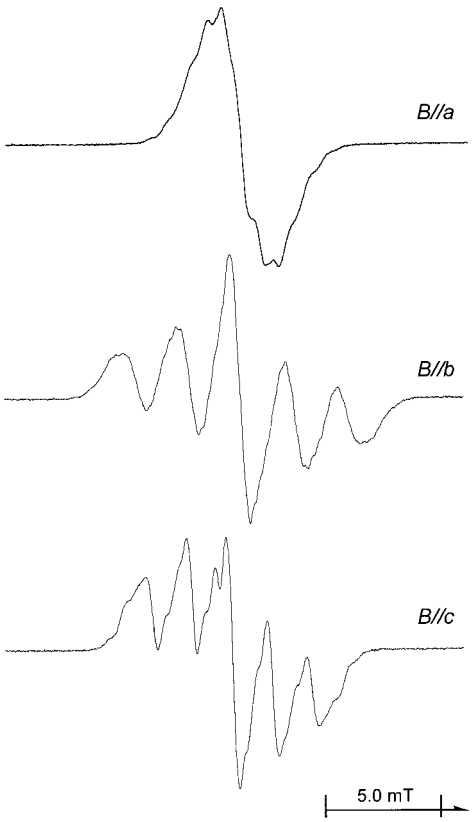

Figure 1. X-band EPR spectra of an X irradiated $Li(N_2D_5)SO_4$ single crystal recorded at 240 K. The external magnetic field is parallel to the *a*, *b*, and *c* crystallographic axes, respectively.

The crystals were irradiated at room temperature for 1 h using an X-ray tube with tungsten anode operated at 70 kV and 20 mA (approximate dose rate 250 Gy/min). The irradiated crystals were mounted to the goniometer head of a Weissenberg X-ray diffraction camera, and the crystallographic axes were aligned with the rotation axis of the camera within 1.0° using oscillation diagrams. The crystals were transferred to a quartz rod for EPR and ENDOR measurements.

X-band EPR and ENDOR spectra were recorded using a Bruker ELEXSYS E580 spectrometer in CW-mode equipped with an EN 801 ENDOR cavity. The ENDOR spectra were obtained with a Bruker E250 ENDOR accessory and an ENI RF 500 amplifier. The RF modulation depth for ENDOR measurements was 190 kHz. A Bruker VT4111 temperature controller using cold nitrogen gas flow regulated the sample temperature. The nitrogen hyperfine and quadrupolar coupling tensors were determined using the program NQENDFIT[13] assuming isotropic *g* tensor. The DFT calculations were performed using the Gaussian 98 program packages[17] on the Cray computer server at the NSC (National Supercomputer Center) in Linköping. The single-point calculation used the B3LYP hybrid functional, and the 6-31G(d,p) basis set based on an optimized structure was evaluated using the MP2 method with the 6-31++G(d,p) basis set, as previously reported.[9]

Results

1. EPR and ENDOR Spectra of the $N_2D_4^{\bullet+}$ Cation. EPR spectra measured along each of the crystallographic axes for X-irradiated LiDzS crystals at room temperature are shown in Figure 1. Because X-irradiation of LiHzS crystals yields the

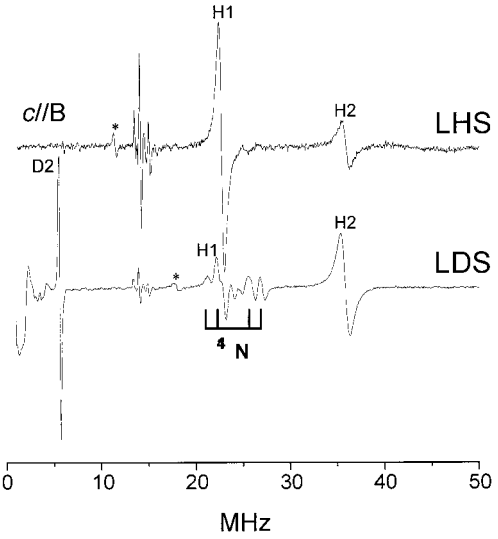

Figure 2. ENDOR spectra obtained from X irradiated $Li(N_2H_5)SO_4$ and $Li(N_2D_5)SO_4$ single crystals. The external magnetic field is parallel to the crystallographic *c* axis.

$N_2H_4^{\bullet+}$ cation,[9] the radical species formed in the LiDzS crystals is expected to be the $N_2D_4^{\bullet+}$ cation. Along the *b* and *c* axes, five lines that are due to the two equivalent nitrogens are observed. This simple spectrum is predicted when the protons of the cation are replaced by deuterons to be the $N_2D_4^{\bullet+}$ species and the hfc is reduced by a factor of 1/6.5. Along the *a* axis, however, an unresolved spectrum appears, because of the small ^{14}N hfc ($a_N = 0.65$ mT). Figure 2 shows the 1−50 MHz ENDOR spectra at 240 K recorded along the *c* axis for LiHzS and LiDzS crystals. It is striking that in the LiDzS crystal the ^{14}N ENDOR lines (marked with a stick diagram in the figure) were clearly observed around 25 MHz (although the low-frequency part of the ^{14}N resonance is partially obscured by the proton signal), whereas these signals were not at all observable in the LiHzS crystal.

The ENDOR spectra obtained with the external magnetic field along each of the crystallographic axes of a LiDzS crystal X irradiated at room temperature and measured at 240 K are shown in Figure 3. Although minor splittings are observed along the *b* and *c* axes because of small misalignments of the crystal, essentially four ^{14}N-ENDOR lines are observed at each axis. This indicates that the two nitrogens in the $N_2D_4^{\bullet+}$ cation are magnetically equivalent. The four ^{14}N-ENDOR lines are ascribed to doublets with splitting virtually equal to twice the ^{14}N nuclear Zeeman frequency (ca. 1.1 MHz) and centered at half the ^{14}N hfc, with each of these doublet lines further split into another doublet by the nqc, i.e., 2 × 2 lines.[13−16] Thus, the four ENDOR transitions are due to

$$m_s:\ |+1/2\rangle,\ m_I:\ |-1\rangle \Leftrightarrow |0\rangle,\ |+1\rangle \Leftrightarrow |0\rangle$$
$$m_s:\ |-1/2\rangle,\ m_I:\ |-1\rangle \Leftrightarrow |0\rangle,\ |+1\rangle \Leftrightarrow |0\rangle \qquad (1)$$

Here the four transitions are denoted as ($+^1/_2$, -1), ($+^1/_2$, $+1$), ($-^1/_2$, -1) and ($-^1/_2$, $+1$), respectively. These first-order ENDOR transitions are to be observed at[13,18]

$$\Delta E = G(m_s) + \frac{P(m_s)}{G^2(m_s)}3(m_I - 1/2) \qquad (2)$$

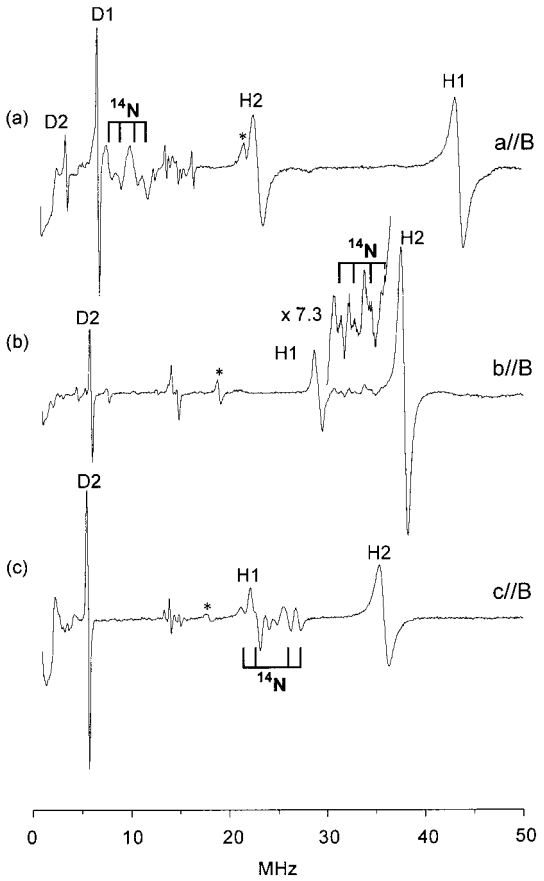

Figure 3. ENDOR spectra of an X irradiated $Li(N_2D_5)SO_4$ single crystal recorded at 240 K with the external magnetic field along the crystallographic *a*, *b*, and *c* axes, respectively. In each case, the field was locked to the center of the corresponding EPR spectrum in Figure 1. The lines marked by * are the 2nd harmonic of a real line because if the nonlinearity of the rf power amplifier.

where

$$G(m_s) = \sqrt{\vec{\eta}\left(\frac{m_s}{g'}\mathbf{g}\cdot\mathbf{T} - \nu_I\mathbf{E}\right)\left(\frac{m_s}{g'}\mathbf{T}\cdot\mathbf{g} - \nu_I\mathbf{E}\right)\vec{\eta}}$$

$$P(m_s) = \vec{\eta}\left(\frac{m_s}{g'}\mathbf{g}\cdot\mathbf{T} - \nu_I\mathbf{E}\right)\mathbf{Q}\left(\frac{m_s}{g'}\mathbf{T}\cdot\mathbf{g} - \nu_I\mathbf{E}\right)\vec{\eta}$$

$$g' = \sqrt{\vec{\eta}\cdot\mathbf{g}\cdot\mathbf{g}\cdot\vec{\eta}} \qquad (3)$$

where $\vec{\eta}$ is the direction of the external magnetic field, **g** is the *g* tensor, **T** is the hyperfine coupling tensor, **Q** is the quadrupolar coupling tensor, ν_I is Larmor frequency of ^{14}N, and **E** is the unit tensor ($E_{ij} = \delta_{ij}$).

The sharp and intense signals at around 5 MHz are attributable to strongly coupled deuterons (D1 and D2). The hfc determined from these lines are perfectly corresponding to 1/6.5 ($=\gamma_D/\gamma_H$) of the strongly coupled protons, supporting the notion that the radical formed in the LiDzS crystal is $N_2D_4^{\bullet+}$. The nqc of ^2D is too small to be observed under the present experimental conditions.

The ENDOR signals of the strongly coupled protons in $N_2H_4^{\bullet+}$ (H1 and H2) were intensely observed even in LiDzS, and the resonance frequencies of the signals are the same as in LiHzS.[9] The presence of these lines is probably due to imperfect deuteration of the crystal. It appears, however, that the ENDOR transitions of the protons are enhanced in the partially deuterated crystals. This is further commented below.

TABLE 1: Orientation of the Symmetry-Determined Coordinate System *XYZ* with Respect to the Unit Cell Axes ⟨*abc*⟩, Calculated from the ^1H hfc Tensor Data Reported in Ref 9

	⟨*a*⟩	⟨*b*⟩	⟨*c*⟩
X	0.2461	−0.7677	−0.5922
Y	−0.5550	0.3870	−0.7364
Z	0.7942	0.5099	−0.3306

2. ENDOR Data Fitting. The ^{14}N-ENDOR lines were observed at most field orientations throughout the three orthogonal planes, <*a*,*b*>, <*b*,*c*>, and <*c*, *a*>. The ENDOR spectra are, however, more complicated than outlined above because of site splitting from the two magnetically inequivalent sites in the orthorhombic crystal. Consequently, a total of two sets of four lines (eight lines) are observed at all orientations except for along the crystallographic axes.

To use the program NQENDFIT,[13] based on eqs 2−3 above, the quantum numbers m_s and transitions $m_I \rightarrow m_I \pm 1$ for each ^{14}N-ENDOR line must be assigned. This is usually accomplished by an educated guess. However, in the present case, the assignment did not become clear until some model calculations had been performed. Therefore, the first step in this process consisted in estimating theoretical hyperfine and quadrupolar tensors for the radical.

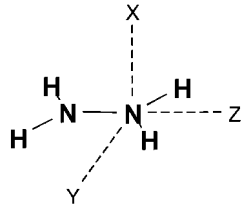

To calculate the ^{14}N-hyperfine coupling and quadrupolar coupling tensors, the orientation of the radical in the unit cell must be known. The proton couplings in the $^{\bullet}N_2H_4^+$ radical were studied by Itagaki et al.[9] On the basis of their observations, the symmetry-determined reference frame ⟨*XYZ*⟩, as defined above, relative to the crystal unit cell system, ⟨*abc*⟩, can be determined and is given in Table 1.

Now, the spin density distribution of the radical was estimated using the SCF RHF/CI INDO MO method.[19] The nitrogen dipolar coupling tensor is mainly due to spin localized in the nitrogen 2p orbitals. The central coupling is mostly from the spin in the $2p_x$ orbital, calculated to be $\rho_{2p_x} = 0.4988$. In addition, small spin densities in the $2p_y$ (0.0086) and $2p_z$ (−0.0014) and the spin in the $2p_x$ orbital at the neighboring nitrogen atom, ρ_α, contribute. The dipolar coupling tensor with unit spin density in ^{14}N 2p orbitals was reported by Morton et al.[20] and employed in this work. When the $2p_x$ orbital is located on a nitrogen atom, the coupling to an α-^{14}N is given by (−1.15, −2.04, 3.18) MHz (calculated with $Z^* = 3.90$, $R = 1.315$ Å, and the nuclear *g* factor for ^{14}N, 0.4038). The isotropic value of the ^{14}N coupling is obtained by scaling the calculated 2s orbital spin density (0.020) with the constant 1811 MHz[20] yielding 36.2 MHz. Together with the dipolar coupling tensor calculated above, the estimated hyperfine coupling tensor is obtained and is given in Table 2 in the experimental frame of reference.

To calculate the ^{14}N-quadrupolar coupling tensors, the method previously described[21] was used. With the ^{14}N nuclear quadrupole moment being $Q = 193 \times 10^{-32}$ m^2,[22] the required factor of proportionality[21] $e^2Q4\pi\epsilon_0 2I(2I-1)ha_0^3$ equals 2.27 MHz. In the literature, values between 2.0 and 2.5 MHz have also been used.[23]

TABLE 2: Theoretically Estimated ^{14}N Hyperfine and Quadrupolar Coupling Tensors for the $N_2H_4^{\bullet+}$ Radical

	principal values (MHz)			eigenvectors		
tensor	*A*	a_{iso}	*B*	⟨*a*⟩	⟨*b*⟩	⟨*c*⟩
^{14}N hfc[a]	90.6		54.4	0.2461	−0.7673	−0.5922
	8.60	36.2	−27.6	0.7942	0.5099	−0.3306
	9.40		−26.8	−0.5550	0.3870	−0.7364
b	79.66		51.31	0.2461	−0.7673	−0.5922
	2.77	28.35	−25.58	0.7942	0.5099	−0.3306
	2.62		−25.73	−0.5550	0.3870	−0.7364
^{14}N nqc[a]	−2.22			0.2461	−0.7673	−0.5922
	0.85			−0.5550	0.3870	−0.7364
	1.37			0.7942	0.5099	−0.3306
b	−1.67			0.2461	−0.7673	−0.5922
	0.10			−0.5550	0.3870	−0.7364
	1.57			0.7942	0.5099	−0.3306
N−N bond direction[c]				0.7942	0.5099	−0.3306
perpendicular to radical plane[c]				0.2461	−0.7673	−0.5922

[a] Calculated as described in text. [b] Calculated from DFT calculations. [c] See Table 1.

The major contribution to the $N_2H_4^{\bullet+}$ radical ^{14}N-quadrupolar coupling is from the electrons distributed over the central nitrogen atoms. The electric field gradient tensor elements from Slater orbitals located at the quadrupole itself were not used in the previous work[21] but are easily evaluated, and the integrals are listed in Appendix 1. The charge density matrix elements $\rho_{\mu\nu}$ of the radical, was found from the SCF RHF/CI INDO MO calculations. The quadrupolar coupling due to the electron density at the central nitrogen atom was calculated to be (−1.87, 0.55, 1.32) MHz, with directions corresponding to the axes of the ⟨*XYZ*⟩ reference frame. In the same basis, the charge density at the remaining part of the molecule contributes with a tensor of (−0.35, 0.20, 0.15) MHz. Adding these contributions gives the calculated quadrupolar coupling tensor shown in Table 2.

The theoretical tensors in Table 2 were now used to calculate the angular variation of the ENDOR transitions of the ^{14}N coupling. The calculated line variation is not particularly close to the experimental data points because of an overestimate of the magnitude of the isotropic hyperfine coupling. However, the calculated variations agree sufficiently close with the data to establish the quantum transition numbers of the four different ENDOR transitions, and in particular, at frequencies above 10 MHz, it was found that the four different ENDOR lines moves in an almost parallel fashion through the planes of rotation. On the basis of this information, it was possible to use the experimental high-frequency ENDOR lines ($m_S = -1/2$ branch) in NQENDFIT[13] and obtain the experimental ^{14}N hyperfine coupling and nuclear quadrupole coupling tensors for the $N_2H_4^{\bullet+}$ radical. At several orientations, the nitrogen hfc's are sufficiently small for the 1st order Weil/Anderson theory[18] to partly break down. Second-order corrections following the theory of Iwasaki[24] were consequently applied throughout. The final tensors are given in Table 3. The solid lines in Figure 4 were calculated from the tensors in Table 3, and the data points included in Figure 4 are those used for the calculation of the tensors. In Figure 4, both the high and low frequency ENDOR transition lines are shown. The observed low frequency lines fit well with calculated line variation based on the tensors of Table 3, calculated from only the high-frequency lines.

Because the quadrupolar tensor is traceless, the sign of the nqc is uncertain at a certain orientation. The assignment of each ENDOR line to one of the four transitions, ($+1/2$, ±1) and ($-1/2$, ±1), at a given orientation depends on the relative signs of hfc and nqc. As previously demonstrated,[14,16] it is experimentally possible to check the given ENDOR line assignments by investigating the relative signs of the hfc and nqc at any specific orientation. This was done at several orientations, and the results agreed with the line assignments obtained from the simulations of the theoretical data as described above.

TABLE 3: Hyperfine and Quadrupole Coupling Tensors for ^{14}N and ^{1}H for the $N_2D_4^{\bullet+}$ and $N_2H_4^{\bullet+}$ Cations Observed at 240 K in $Li(N_2D_5)SO_4$ and $Li(N_2H_5)SO_4$ Crystals, Respectively, X Irradiated at 295 K

	principal values (MHz)			eigenvectors		
tensor	*A*	a_{iso}	*B*	⟨*a*⟩	⟨*b*⟩	⟨*c*⟩
^{14}N hfc	81.56		49.70	0.210	−0.781	−0.588
	7.50	31.86	−24.36	0.055	0.610	−0.791
	6.53		−25.33	−0.976	−0.134	−0.171
^{14}N nqc	−1.228			0.406	−0.595	−0.693
	0.357			−0.830	−0.557	−0.008
	0.871			0.381	−0.579	0.721
^{1}H hfc[a]	−59.64		−28.07	0.406	0.647	−0.645
A	−37.34	−31.57	−5.77	0.234	−0.756	−0.611
	2.28		33.85	0.883	−0.097	0.459
^{1}H hfc[a]	−59.64		−28.07	−0.963	−0.255	−0.087
B	−37.34	−31.57	−5.77	0.258	−0.779	−0.572
	2.28		33.85	−0.078	0.573	−0.816
N−N bond direction[b]				0.7942	0.5099	−0.3306
perpendicular to radical plane[b]				0.2461	−0.7673	−0.5922

[a] Ref 9. [b] See Table 1.

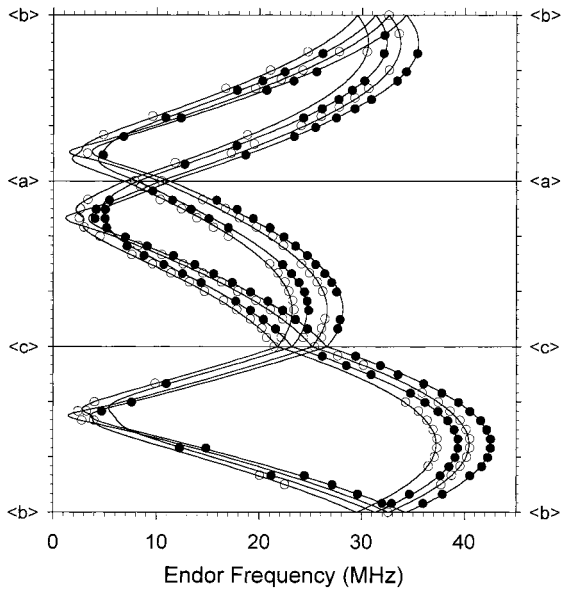

Figure 4. ●, −: The experimental high-frequency ($m_s = -1/2$) ^{14}N ENDOR data from the $N_2D_4^{\bullet+}$ cation. The solid curves represent the calculated angular variations from the hfc and nqc tensors in Table 3. Only the experimental data indicated with solid circles (●) were used for the evaluation of the ^{14}N-hfc and nqc tensor parameters in the table.

Discussion

1. ^{14}N hfc and nqc Tensors of the $N_2H_4^{\bullet+}$ Cation. The ^{14}N hfc of the $N_2D_4^{\bullet+}$ radical cation (Table 3) is nearly axially symmetric and is very close to that of the $N_2H_5HC_2O_4$ single crystal (77.3, 7.0, 7.0 MHz) previously reported by EPR.[11] The hfc of the ^{14}N and ^{1}H nuclei have one common tensor axis for the values of +81.54 and −37.34 MHz, respectively, which is the perpendicular to the molecular plane. This supports the planar structure of the $N_2H_4^{\bullet+}$ cation. The overall agreement with the two theoretically estimated ^{14}N hfc tensors in Table 2 is very good. In particular it is clear that the spin densities of the $2p_z$ orbitals at the ^{14}N nuclei are each about 0.5, confirming

that the unpaired electron in the cation is predominantly shared on the $2p_z$ orbital of the two equivalent ^{14}N atoms of a π^* planar radical.

The experimental ^{14}N nqc exhibited a rhombic symmetry with a fairly large asymmetry parameter $\eta = 0.42$; the asymmetry parameter is defined by McDowell and Naito[25] as $(Q_{aa} - Q_{bb})/Q_{cc}$ with $|Q_{aa}| < |Q_{bb}| < |Q_{cc}|$. A rhombic symmetry of the nqc tensor was also predicted by the theoretical calculations (Table 2).

The eigenvectors for the experimentally determined nqc tensor (Table 3) are very close to the symmetry-determined axis system *XYZ*. In particular, the direction for the largest negative value deviates only about 15° from the perpendicular to the radical, the predicted direction according to the theoretical calculations in Table 2. The corresponding eigenvalue is somewhat smaller than that calculated.

Considering the eigenvectors for the two positive principal values of the nqc tensor, however (Table 3), it appears that an interchange has taken place as compared with the theoretical tensors in Table 2. Thus, experimentally, the smallest positive principal value occurs close to the N−N bond direction (designated *Z*), whereas both theoretical calculations predict the corresponding value to occur along *Y*. A closer examination of the theoretical methods reveals that, in fairly symmetric molecules such as $N_2H_4^{\bullet+}$, the relative magnitudes of the two positive nqc tensor principal values is determined mainly by the electron densities of the in-plane 2p orbitals ($2p_y$ and $2p_z$) at the quadrupolar nucleus. Small deviations from ideal symmetry will result in small changes in these charge densities. Our calculations indeed showed that very small differences in charge densities of the in-plane 2p orbitals result in considerable deviations from the ideal case for the nqc tensor. Two alternative explanations for the differences between theory and experiment (Tables 2 and 3) are then (a) the computational methods (SCF RHF/CI INDO and DFT) have not been able to reproduce the correct in-plane charge distribution of the (isolated) radical or (b) environmental interactions produce minor perturbations to the radical geometry and hence change the charge distributions. These changes are not recognized by the gas-phase molecular orbital calculations presented here.

It is in this context of interest to note that, in an ENDOR study of the tempone nitroxide radical, Brustolon et al.[16] found that the smallest positive quadrupolar coupling occurred close to the >N−O bond direction, the direction corresponding to the >N−N< bond direction (*Z*) in the present work. Our DFT calculations on a simplified nitroxide radical, $(CH_3)_2N-O^{\bullet}$, being slightly unsymmetrical because of different conformations of the two methyl groups, nicely reproduced the experimental nqc tensor. On the other hand, the SCF RHF/CI INDO based method yielded a good value along *X* but interchanged the two positive *Y* and *Z* values, similar to the case of $N_2H_4^{\bullet+}$. The two computational methods assess the in-plane charge densities slightly differently. Hence, care should be exercised when doing theoretical calculations of nqc tensors for small, symmetric radicals, as this experimental parameter is much more sensitive to very small differences in p orbital charge densities than other magnetic properties measured by EPR/ENDOR methods.

2. ^{14}N-ENDOR Enhancement in the Deuterated Crystal. As described above, ^{14}N-ENDOR signals were observed in the LiDzS crystal, which could not be detected in the LiHzS system.[9] It is evident that the deuterium substitution made it possible to observe the ^{14}N-ENDOR signals. Relaxation caused by modulation of the ^1H hyperfine interaction in LiHzS is expected to be slower in LiDzS by the factor 1/6.5 (γ_D/γ_H).[26] This mechanism does not directly affect the ^{14}N-ENDOR intensity, however, suggesting that the nuclear ^{14}N-^1H dipole−dipole interaction has a significant contribution to spin−lattice relaxation mechanism in LiHzS. In the LiDzS crystal, the interaction will be reduced approximately by 1/6.5 factor to increase the T_{1n} nuclear relaxation time. That is, the spin system becomes easier to saturate so as to enhance the cw-ENDOR intensity. Ratcliffe[27] investigated the NMR spin−lattice relaxation in various $N_2H_6^+$ salts such as $N_2H_6SO_4$ and suggested that the $^{14}N-^1H$ dipole−dipole interaction in the $-NH_3^+$ groups made a contribution of ca. 14% to the maximum relaxation rate.

The apparent ENDOR enhancement of the unsubstituted protons in the $N_2D_4^{\bullet+}$ radical can be the result of a similarly weakened proton−proton dipolar interaction in the H−D-containing species resulting in ENDOR enhancement through a reduced proton T_{1n} relaxation rate.

Conclusions

The ^{14}N-ENDOR signals of a hydrazine radical cation ($N_2D_4^{\bullet+}$ and/or its other ^1H isotopomeric species) were observed in single crystals of deuterated lithium hydrazinium sulfate after X irradiation. Corresponding ENDOR signals were not observed in protonated crystals.[9] The hfc and nqc tensors of the nitrogenes were successfully determined. The hfc tensor obtained for the two equivalent ^{14}N atoms is very close to that reported in a $N_2H_5HC_2O_4$ single crystal, and the present results support the previous conclusion that the cation has a planar structure at 240 K and also confirmed the radical reorientation. The experimentally obtained nqc tensor showed a rhombic symmetry tensor, and the eigenvectors were evaluated to be very close to the molecular axes shown in the text, supporting the planar structure of $N_2D_4^{\bullet+}$ at 240 K. The apparent ENDOR enhancement for the ^{14}N signals by the deuterium substitutions may be ascribed to the reduction in dipole−dipole interactions between two protons which increase the T_{1n} relaxation time.

Acknowledgment. This work was supported by NFR (Swedish National Science Research Council), STINT (The Swedish Foundation for Institutional Cooperation in Research and Higher Education), and NorFa (Nordic Academy for Advanced Studies). We thank to Prof. M. Brustolon for kindly giving us valuable comments on this work.

Appendix 1

When the electron orbitals at a ^{14}N atom are described using Slater orbitals, it is possible to calculate the contributions to each element of the quadrupolar coupling tensor, Q_{ij}, from every electron. The necessary integrals for doing this are given below and in a previous work.[21]

The Slater orbitals are given by

$$|1s\rangle = \left[\frac{\zeta^3}{\pi}\right]^{1/2} e^{-\rho}|2p_x\rangle = \left[\frac{\zeta^3}{\pi}\right]^{1/2} \rho e^{-\rho} \cos\theta$$

$$|2s\rangle = \left[\frac{\zeta^3}{3\pi}\right]^{1/2} \rho e^{-\rho}|2p_y\rangle = \left[\frac{\zeta^3}{\pi}\right]^{1/2} \rho e^{-\rho} \sin\theta \cos\phi$$

$$|2p_z\rangle = \left[\frac{\zeta^3}{\pi}\right]^{1/2} \rho e^{-\rho} \sin\theta \sin\phi \qquad (4)$$

where $\zeta = z^*/a_0 n$ and $\rho = \zeta r$, with Z^* being the effective nuclear charge, n the principal quantum number, and a_0 the Bohr radius.

The coordinates used in the calculations on the $N_2H_4^{\bullet+}$ radical are defined with the *z* axis along the N−N bond and the *x* axis parallel with the LEO. The Cartesian coordinates with origin

at N may be expressed by (r, θ, ϕ), the polar coordinates with origin at the nucleus at which the orbital is centered

$$x = \frac{\rho}{\zeta}\sin\theta\cos\phi$$

$$y = \frac{\rho}{\zeta}\sin\theta\sin\phi$$

$$z = \frac{\rho}{\zeta}\cos\theta \qquad (5)$$

Defining $P_{ij} = (3x_ix_j - \delta_{ij}r^2)/r^5$, where $i = x$, y, or z and $j = x$, y, or z, yields the nonzero integrals

$$\langle 2p_i|P_{ii}|2p_i\rangle = -\frac{1}{2}\langle 2p_i|P_{jj}|2p_i\rangle = \frac{4\zeta^3}{15} \qquad i \neq j \qquad (6)$$

$$\langle 2p_i|P_{jj}|2p_j\rangle = \frac{\zeta^3}{5} \qquad i \neq j \qquad (7)$$

References and Notes

(1) Vanderkooy, J.; Cuthbert, J. D.; Petch, H. E. *Can. J. Phys.* **1964**, *42*, 1871.
(2) Schmidt, V. H.; Drumheller, J. E.; Howell, F. L. *Phys. Rev. B* **1971**, *4*, 4582.
(3) Howell, L. *Phys. Rev.* **1971**, *4*, 4582.
(4) Anderson, M. R.; Brown, I. D. *Acta Crystallogr. B* **1974**, *30*, 831.
(5) Morawski, P.; Hoffmann, S. K.; Hilczer, W.; Goslar, J. *Acta Phys. Pol. A* **1997**, *91*, 1121.
(6) Goslar, J.; Hilczer, W.; Morawski, P. *Solid State Ionics* **2000**, *127*, 67.
(7) Knispel, R. R.; Petch, H. E. *Can. J. Phys.* **1970**, *49*, 870.
(8) Hilczer, B.; Pukacka, M.; Sabat, A. *Fiz. Dielectr. Radiospectr.* **1979**, *6*, 69.
(9) Itagaki, Y.; Kadam, R. M.; Lund, A.; Sagstuen, E.; Goslar, J. *Phys. Chem. Chem. Phys.* **2000**, *2*, 37.
(10) Edlund, O.; Lund, A.; Nilsson, Å. *J. Chem. Phys.* **1968**, *49*, 749.
(11) Sagstuen, E.; Awadelkarim, O.; Lund, A.; Masiakowski, J. *J. Chem. Phys.* **1986**, *85*, 3223.
(12) Cuthbert, J. D.; Petch, H. E. *Can. J. Phys.* **1963**, *41*, 1629.
(13) Sørnes, A. R.; Sagstuen, E.; Lund, A. *J. Phys. Chem.* **1995**, *99*, 16867.
(14) Sanderud, A.; Sagstuen, E. *J. Phys. Chem.* **1996**, *100*, 9545.
(15) Nelson, W. H.; Atwater, F. M.; Gordy, W. *J. Chem. Phys.* **1974**, *61*, 4726.
(16) Brustolon, M.; Maniero, A. L.; Corvaja, C. *Mol. Phys.* **1984**, 1269.
(17) Frisch, M. J.; Trucks, G. W.; Schlegel, H. B.; Scuseria, G. E.; Robb, M. A.; Cheeseman, J. R.; Zakrzewski, V. G.; Montgomery, J. A., Jr.; Stratmann, R. E.; Burant, J. C.; Dapprich, S.; Millam, J. M.; Daniels, A. D.; Kudin, K. N.; Strain, M. C.; Farkas, O.; Tomasi, J.; Barone, V.; Cossi, M.; Cammi, R.; Mennucci, B.; Pomelli, C.; Adamo, C.; Clifford, S.; Ochterski, J.; Petersson, G. A.; Ayala, P. Y.; Cui, Q.; Morokuma, K.; Malick, D. K.; Rabuck, A. D.; Raghavachari, K.; Foresman, J. B.; Cioslowski, J.; Ortiz, J. V.; Stefanov, B. B.; Liu, G.; Liashenko, A.; Piskorz, P.; Komaromi, I.; Gomperts, R.; Martin, R. L.; Fox, D. J.; Keith, T.; Al-Laham, M. A.; Peng, C. Y.; Nanayakkara, A.; Gonzalez, C.; Challacombe, M.; Gill, P. M. W.; Johnson, B. G.; Chen, W.; Wong, M. W.; Andres, J. L.; Head-Gordon, M.; Replogle, E. S.; Pople, J. A. *Gaussian 98*, revision A.9; Gaussian, Inc.: Pittsburgh, PA, 1998.
(18) Weil, J. A.; Anderson, J. H. *J. Chem. Phys.* **1961**, *35*, 1410.
(19) Oloff, H.; Hüttermann, J. *J. Magn. Reson.* **1980**, *40*, 415.
(20) Morton, J. R.; Preston, K. F. *J. Magn. Reson.* **1978**, *30*, 577.
(21) Sanderud, A.; Sagstuen, E.; Itagaki, Y.; Lund, A. *J. Phys. Chem. A* **2000**, *104*, 6372.
(22) Weil, J. A.; Rao, P. S. *Bruker EPR/ENDOR Frequency Table*; Bruker: Karlsruhe, Germany, 2000.
(23) Schweiger, A. *Struct. Bonding* **1982**, 51.
(24) Iwasaki, M. *J. Magn. Reson.* **1974**, *16*, 417.
(25) McDowell, C. A.; Naito, A. *J. Magn. Reson.* **1981**, *45*, 205.
(26) Atherton, N. M. *Principles of Electron Spin Resonance*; Ellis Horwood: New York, 1993.
(27) Ratcliffe, C. I. *J. Magn. Reson.* **1980**, *38*, 283.